

# Energy Window Augmented Plane Waves Approach to Density Functional Theory

Garry Goldstein

*garrygoldsteinwinnipeg@gmail.com*

In this work we present a new method for basis set generation for electronic structure calculations of crystalline solids. This procedure is aimed at applications to Density Functional Theory (DFT). In this construction, Energy Window Augmented Plane Waves (EWAPW), we take advantage of the fact that most DFT calculations use a convergence loop in order to obtain the self consistent eigenstates of the final (converged) Kohn Sham (KS) Hamiltonian. Here we propose that, for the basis used at each step of the self consistency iteration, we use the previous eigenstate basis, in the interstitial region, and augment it, inside each Muffin Tin (MT) sphere, with the solution to the spherically averaged KS Hamiltonian for the linearization energy of the energy window which contains the energy of that previous eigenstate. Indeed, to reduce the number of times the spherically averaged KS potential needs to be solved inside the MT spheres it is advantageous break up the spectrum into non-overlapping intervals, windows, and solve the spherically averaged KS Hamiltonian inside the MT region only once per window per angular momentum channel (at the linearization energy relevant to that window, usually near the middle of the window). For practical applications it is reasonable to have on the order of five to fifty windows. At each step of the iteration of the solution of the KS equations the EWAPW basis is that of near eigenstates of the KS Hamiltonian for that iteration. Overall the basis size is the comparable with the Augmented Plane Waves (APW) basis set but the number of radial wavefunctions is comparable or greater to Linearized Augmented Plane Waves + Local Orbitals + Higher Derivative Local Orbitals + High Energy Local Orbitals (LAPW+LO+HDLO+HELO) basis set.

## I. INTRODUCTION

The usefulness of a basis set for all electron calculations of crystalline solids within Density Functional Theory (DFT) methods is mainly determined by 1) its linearization error (that is energy errors for eigenstates of the Kohn Sham (KS) Hamiltonian inside the valence band), 2) its ability to handle semi-core states - that is the situation when there is more than one relevant band (not just the valence band) just at or below the Fermi energy, 3) the effectiveness with which the basis set converges to the energy obtained in the infinite basis limit as a function of the number of basis elements for the solution of the KS equations,  $N_{tot}$  - or how hard or soft the basis is, 4) the efficiently with which one can write down the KS Hamiltonian in that basis, amongst other things [1–3]. There are now several known competitors, in the literature, for which basis set is optimal. These can be divided into mostly plane wave basis methods [1–10] and mostly Muffin Tin (MT) basis sets [2, 4, 10–16]. In this work we focus on the plane wave methods [1–9]. Nominally (without augmentation or pseudization), within the plane wave method, the basis set is very simple but is extremely inefficient at obtaining good eigenstates of the KS Hamiltonian for reasonably small wave vector cutoffs - is extremely hard. Indeed near the nuclei, where the electron density is high and highly concentrated (oscillating), the KS potential has high wave vector components so that the eigenstates of the KS Hamiltonian have high wave vector components as well. This means that impractically large numbers of plane waves are needed to accurately describe the environment near atomic nuclei, making the situation generically numerically impossible. There are two main approaches to cure this problem -

that is still use mainly plane wave basis sets: pseudopotentials [2, 3, 17, 18] and augmentation methods [2, 4, 7–10, 19–22]. In this work we focus on augmentation methods.

In augmentation methods the main idea is to divide the crystalline material into two regions: the MT region and the interstitial (IR) region. The MT region is a set of non-overlapping spheres centered at the nuclear coordinates  $\mathbf{r}_\alpha$  with radii  $S_\alpha$  (where  $\alpha$  labels the nuclei). The interstitial region is the rest of the crystal. In the interstitial region a good basis for the solutions of the KS problem are plane waves - as the KS potential is varying slowly with position. In the MT region a good basis for the KS problem is the solutions to the radially averaged KS potential near each nucleus:

$$\begin{aligned} \left[ -\frac{d^2}{dr^2} + \frac{l(l+1)}{r^2} + \bar{V}_{KS}^{n\alpha}(r) \right] r u_{l\alpha}^n(r, E) = \\ = E r u_{l\alpha}^n(r, E) \end{aligned} \quad (1)$$

and  $\bar{V}_{KS}^{n\alpha}(r)$  is the spherically average (KS) potential inside the  $\alpha$ 'th MT sphere,  $n$  is the iteration of the solution to the KS equations (added into the conventional notation for later convenience),  $r = |\mathbf{r} - \mathbf{r}_\alpha|$  is the distance from the center of the MT sphere and  $E$  is the energy. We note that the electron mass has been set to 1/2. The key question is what energy,  $E$ , to use in the solutions of Eq. (1) when glueing it to the plane waves in the interstitial.

An early solution to the glueing problem due to Slater was simply to chose the linearization in the middle of the valence band and augment with plane waves to obtain the following APW basis  $\phi_{\mathbf{k}\mathbf{G}}^n(E^n) =$ :

$$\begin{cases} \frac{1}{\sqrt{\Omega}} \exp(i(\mathbf{k} + \mathbf{G}) \cdot \mathbf{r}) & \mathbf{r} \in IR \\ \sum_{lm} A_{\mathbf{k}\mathbf{G}}^{lm\alpha n} u_{l\alpha}^n(r, E^n) Y_{lm}(\widehat{\mathbf{r} - \mathbf{r}_\alpha}) & \mathbf{r} \in MT_\alpha \end{cases} \quad (2)$$

Where  $E^n$  is the  $n$ 'th iteration linearization energy,  $IR$  is the interstitial,  $MT_\alpha$  is the  $\alpha$ th MT sphere,  $\Omega$  is the volume of the unit cell,  $\mathbf{k}$  is a point in the first Brillouin,  $\mathbf{G}$  is a reciprocal lattice vector,  $Y_{lm}$  are spherical

harmonics, and  $A_{\mathbf{k}\mathbf{G}}^{lm\alpha n}$  are the matching coefficients that insure the wavefunction is continuous. Furthermore the  $A_{\mathbf{k}\mathbf{G}}^{lm\alpha n}$  can be computed using the relation [23]:

$$\frac{1}{\sqrt{\Omega}} \exp(i(\mathbf{k} + \mathbf{G}) \cdot \mathbf{r}) = \frac{4\pi}{\sqrt{\Omega}} \exp(i(\mathbf{k} + \mathbf{G}) \cdot \mathbf{r}_\alpha) \times \sum_{l,m} Y_{lm}^* \left( \widehat{\mathbf{k} + \mathbf{G}} \right) Y_{lm} \left( \widehat{\mathbf{r} - \mathbf{r}_\alpha} \right) i^l j_l (|\mathbf{k} + \mathbf{G}| |\mathbf{r} - \mathbf{r}_\alpha|) \quad (3)$$

which decouples the matching problem into separate angular momentum channels. Here  $j_l$  are the spherical Bessel functions. There is a cutoff  $l_{max} \sim 8 - 12$ , which comes about because of the negligibly small values of the spherical Bessel functions, for large  $l$ , inside the MT spheres. This is not an efficient solution because of the large linearization errors for the wavefunction. Alternatively it is possible to choose  $E^n$  self consistently that is the same as every eigenvalue for each eigenwavefunction (however that is very numerically demanding) [1, 2].

Another solution to this glueing problem is the Linearized Augmented Plane Waves (LAPW) basis set [1, 2, 4]. Here plane waves are augmented within the

MT sphere by a linear combination of the solutions to the spherically averaged KS Hamiltonian (see Eq. (1)) at the linearization energy  $E_L^n$  (typically the middle of the valence band)  $u_{l\alpha}^n(r, E_L^n)$  and its derivative with respect to energy  $\dot{u}_{l\alpha}^n(r, E_L^n) = \frac{\partial}{\partial E} u_{l\alpha}^n(r, E_L^n)$ . This is done for all angular momentum channels  $lm$  (up to  $l_{max}^L$ ) and all atoms  $\alpha$ . Whereby, by matching the MT wavefunctions to the plane wave wavefunction, that is demanding the total function be continuous and continuously differentiable - at the MT sphere radius [1, 2, 4-6] - we obtain a efficient continuously differentiable basis set. The LAPW basis set may be written as:

$$\phi_{\mathbf{k}\mathbf{G}}^{Ln}(E_L^n) = \begin{cases} \frac{1}{\sqrt{\Omega}} \exp(i(\mathbf{k} + \mathbf{G}) \cdot \mathbf{r}) & \mathbf{r} \in IR \\ \sum_{lm} [a_{\mathbf{k}\mathbf{G}}^{lm\alpha n} u_{l\alpha}^n(r, E_L^n) + b_{\mathbf{k}\mathbf{G}}^{lm\alpha n} \dot{u}_{l\alpha}^n(r, E_L^n)] Y_{lm} \left( \widehat{\mathbf{r} - \mathbf{r}_\alpha} \right) & \mathbf{r} \in MT_\alpha \end{cases} \quad (4)$$

Where  $a_{\mathbf{k}\mathbf{G}}^{lm\alpha n}$  and  $b_{\mathbf{k}\mathbf{G}}^{lm\alpha n}$  are the matching coefficients that insure the wavefunction is continuous and continuously differentiable. Furthermore  $a_{\mathbf{k}\mathbf{G}}^{lm\alpha n}$  and  $b_{\mathbf{k}\mathbf{G}}^{lm\alpha n}$  can be computed using the relation in Eq. (3). This allows for efficient description of the valence band which is adjustable to the form of the KS potential near the nuclei. This idea can be extended to Linearized Augmented Lattice Adapted Plane Waves ((LA)<sup>2</sup>PW) which have the form [19]:

$$\phi_{\mathbf{k}\mathbf{G}}^n(E_L^n) = \sum_{\mathbf{G}} o_{\mathbf{k}\mathbf{G}}^{nj} \phi_{\mathbf{k}\mathbf{G}}^n(E_L^n) \quad (5)$$

(here  $j$  labels a basis element). Where one choice for  $o_{\mathbf{k}\mathbf{G}}^{nj}$  is given Basis of Early Eigenfunctions  $BEE - (LA)^2 PW$  where one introduces the solutions to the KS equations [19]:

$$\psi_\nu^n = \sum z_{\mathbf{k}\mathbf{G}}^{\nu n} \phi_{\mathbf{k}\mathbf{G}}^n(E_L^n) \quad (6)$$

and

$$o_{\mathbf{k}\mathbf{G}}^{nj} = z_{\mathbf{k}+\mathbf{G}}^{\nu 1} \quad (7)$$

for  $\nu = j$ . One then truncates the basis set with number of basis functions  $j \ll N_{\mathbf{G}}$  (where  $N_{\mathbf{G}}$  is the number of reciprocal lattice points), as one has a basis of near eigenvectors in the IR, and runs the KS loop to convergence. This greatly reduces the basis set size needed for the iterative calculations after the first iteration [19]. These methods can be further improved as in Quadratically Augmented Plane Waves QAPW [21, 22] where  $\ddot{u}_{l\mu}^n(r, E_L^n) = \frac{\partial^2}{\partial E^2} u_{l\mu}^n(r, E_L^n)$  is also used inside the MT sphere and one more derivative (with respect to the radial co-ordinate) is matched to the plane waves in the IR which reduces linearization errors. However, the more derivatives are matched the more the radial wavefunction inside the MT sphere look like Bessel functions (indeed in the limit where an infinite number of derivatives is matched the radial wavefunction must be exactly Bessel) the higher cutoff, the harder the basis becomes [7, 19]. Furthermore if there are several relevant bands one can use Local Orbitals (LO) basis wave functions [1, 7-9, 19, 24]. Many LO like basis wavefunctions are of the form:

$$\phi_{LO}^{nlm\alpha} = \begin{cases} 0 & \mathbf{r} \in IR, MT_\beta \text{ for } \beta \neq \alpha \\ [\bar{a}^{l\alpha n} u_{l\alpha}^n(r, E_L^n) + \bar{b}^{l\alpha n} \tilde{u}_{l\alpha}^n(r, E_L^n) + \bar{c}^{l\alpha n} \tilde{u}_{l\alpha}^n(r)] Y_{lm}(\widehat{\mathbf{r} - \mathbf{r}_\alpha}) & \mathbf{r} \in MT_\alpha \end{cases} \quad (8)$$

Where the wavefunction is chosen to be continuous and continuously differentiable using the coefficients  $\bar{a}^{l\alpha n}$ ,  $\bar{b}^{l\alpha n}$  and  $\bar{c}^{l\alpha n}$ . There are many choices for  $\tilde{u}_{l\alpha}^n$ . For regular LO these are chosen as  $\tilde{u}_{l\alpha}^n(r) = u_{l\alpha}^n(r, E_{SC}^n)$  where  $SC$  stands for semicore states. For Higher Derivative Local Orbitals [7, 19, 24–26] (HDLO)  $\tilde{u}_{l\alpha}^n = \ddot{u}_{l\alpha}^n(r, E_L^n)$ , while for Higher Energy Local Orbitals [7, 19, 24–26] (HELO) the  $\tilde{u}_{l\alpha}^n$  is an eigenstate of the spherically averaged KS Hamiltonian (inside  $MT_\alpha$ ) with energy  $E_{HELO}^{nl}$

such that

$$D_{l,k}^{n\alpha} \equiv \frac{S_\alpha \frac{\partial}{\partial r} \tilde{u}_{l\alpha}^n(S_\alpha, E_{HELO}^{nl})}{\tilde{u}_{l\alpha}^n(S_\alpha, E_{HELO}^{nl})} = -(l+1) \quad (9)$$

Where  $\frac{\partial}{\partial r}$  is the radial derivative. This is chosen to make  $\phi_{LO}^{nl\alpha}$  orthogonal to each other and to the core states. Several HELO bands are possible. This method, LAPW+LO+HDLO+HELO greatly improves the accuracy of the electronic structure method.

A competitor to the LAPW method is the APW+lo method which uses the basis in Eq. (2) and augments it with lo wavefunctions of the form:

$$\phi_{lo}^{nlm\alpha} = \begin{cases} 0 & \mathbf{r} \in IR, MT_\beta \text{ for } \beta \neq \alpha \\ [a_{lo}^{l\alpha n} u_{l\alpha}^n(r, E^n) + b_{lo}^{l\alpha n} \tilde{u}_{l\alpha}^n(r, E^n)] Y_{lm}(\widehat{\mathbf{r} - \mathbf{r}_\alpha}) & \mathbf{r} \in MT_\alpha \end{cases}$$

where the coefficients  $a_{lo}^{l\alpha n}$  and  $b_{lo}^{l\alpha n}$  are chosen to make the wavefunction continuous. These additional wavefunctions [9, 27, 28] which often come in a very small number of angular momentum channels [9, 27, 28] lead to a linearization of the APW basis set.

In this work we will not be proposing any new type of LO (such as HDLO or HELO or conventional LO). As a matter of fact Energy Window Augmented Plane Wave (EWAPW) can be viewed as a competitor to the various forms of LO and lo, as we argue that LO and lo type wavefunctions will not significantly improve the accuracy of the basis set to obtain the eigenstates of the KS Hamiltonian (see Section III G). Indeed, all of our basis, EWAPW, wavefunctions will be of the form  $\frac{1}{\sqrt{\Omega}} \sum_{\mathbf{G}} \bar{o}_{\mathbf{k}\mathbf{G}}^{nj} \exp(i(\mathbf{k} + \mathbf{G}) \cdot \mathbf{r})$  in the IR, for appropriate  $\bar{o}_{\mathbf{k}\mathbf{G}}^{nj}$  as in  $(LA)^2 PW$ . However, unlike  $(LA)^2 PW$  methods, inside the MT region we will also be modifying the linearization energy of the  $j$ 'th basis element based on the eigenvalue information from the previous,  $n-1$ 'st, iteration of the solution of the KS equations. More precisely  $\bar{o}_{\mathbf{k}\mathbf{G}}^{nj}$  will be chosen so that in the IR the basis wavefunctions have the same plane wave expansion as eigenstates  $\nu$  of the previous iterations with  $\nu = j$ . In the MT we will be augmenting these wavefunction at the energies  $E_j^n$  which are nearly equal to the eigenenergies of the previous iteration  $\varepsilon_{\mathbf{k}\nu}^{n-1}$  (with  $j = \nu$ ) except we will be using a widowing function  $\mathcal{E}_w^n(E)$  (which is a piecewise constant approximation to the identity function:  $Id(E) = E$ , see Fig. (1)) and linearizing (augmenting) at  $E_j^n = \mathcal{E}_w^n(\varepsilon_{\mathbf{k}\nu}^{n-1}) \cong \varepsilon_{\mathbf{k}\nu}^{n-1}$ . As such one needs solve

the spherically averaged KS Hamiltonian at a discrete (on the order of five to fifty) number of values  $\mathcal{E}_w^n(E)$  takes on - per angular momentum channel, making it practical. Furthermore as we are able to have many linearization energies the method is likely more accurate than APW+lo or LAPW (comparable to LAPW+LO+HDLO+HELO), however we do not increase the basis size beyond APW levels. Detailed derivations are given in Section II below. We now note that the numerical efficiency of a DFT calculation is often determined by the diagonalization time and the time it takes to numerically set up the KS Hamiltonian and charge density [29]. Overall EWAPW has roughly the same diagonalization time as APW (same size of basis) but takes a comparable amount of time to set up the charge density and KS Hamiltonian as LAPW+LO+HDLO+HELO as it has a comparable number of radial basis functions. We note that in many situations with a large basis set the diagonalization time is the biggest [29].

The rest of this paper is organized as follows. In Section II A we write down the EWAPW wavefunctions in several equivalent ways. This is the main result of this work. In Section II B we show how to incorporate EWAPW wavefunctions into a KS loop. In Section III we will discuss various technical details needed to make the procedure possible on modern computers as well as some technical comments useful for computational efficiency. In Section IV we present technical steps to write down the KS Hamiltonian, overlap and electron density, this is highly similar to regular Full Potential Linearized

Augmented Plane Waves (FLAPW). In Section V we conclude. Various extensions are considered in the Appendices.

## II. MAIN EXPLANATIONS

### A. Wavefunctions

We now describe in detail the wavefunctions used in the EWAPW basis. EWAPW is a method to solve the question of which energy  $E$  can be used to glue the wavefunction  $u_{l\alpha}^n(E)$  in the MT to which combination of plane waves in the IR. This is done using information from the previous iteration of the solutions to the KS equations. We will not be using and LO/lo (or HDLO or HELO etc.) wavefunctions and the basis set size, per  $\mathbf{k}$  point, will be the same as the number of reciprocal lattice vectors  $N_{\mathbf{G}}$  (or less see Section III D). We will also avoid solving for the radially averaged KS equation (see Eq. (1)) at every energy  $\varepsilon_{\mathbf{k}\nu}^n$  (which is impractically hard) by using a windowing function  $\mathcal{E}_w^n(E)$  that maps nearly via the identity into a small discrete set of values  $\varepsilon_{\mathbf{k}\nu}^n \rightarrow E_{i,n}^V$  (see Fig. (1)) and only solving Eq. (1) at the energy values  $E_{i,n}^V$ .

We begin with a definition of a windowing function  $\mathcal{E}_w^n(E)$ , which is given by:

$$\mathcal{E}_w^n(E) = \sum_{i=2}^N E_{i,n}^V \cdot (\Theta(E - E_{i-1,n}^U) - \Theta(E - E_{i,n}^U)) \quad (10)$$

Where  $E_{1,n}^U = -\infty$ ,  $E_{N,n}^U = +\infty$  and  $E_{i-1,n}^U < E_{i,n}^U < E_{i,n}^V \forall i$ . Here  $\Theta$  is the Heaviside function. Here  $N - 1$ , on the order of five to fifty, is the number of windows. The windowing function is a piecewise constant approximation to the identity function  $Id(E) = E$ . A typical  $\mathcal{E}_w^n(E)$  is pictured in Fig. (1). We note that, as we shall see below, we will only need to solve Eq. (1) for the energies  $E_{i,n}^V$ . We further note that the windowing function divides the spectrum into non-overlapping intervals, windows,  $E_{i-1,n}^U \leq E < E_{i,n}^U$  and assigns each window the value  $E \rightarrow E_{i,n}^V$ . Some methods to obtain  $E_{i,n}^V$  and  $E_{i,n}^U$

are described in Section (III H). Here we simply note that, in general, it is advantageous to place many  $E_{i,n}^U$  in the energy range of the valence and semicore bands (as such approximating the identity more accurately in those crucial regions) and a few for the rest of the spectrum (which is less crucial). We now introduce the wavefunctions:  $\Phi_{\mathbf{k}\mathbf{G}}^n(E) =$

$$\begin{cases} \frac{1}{\sqrt{\Omega}} \exp(i(\mathbf{k} + \mathbf{G}) \cdot \mathbf{r}) & \mathbf{r} \in IR \\ \sum_{lm} \bar{A}_{\mathbf{k}\mathbf{G}}^{lm\alpha n}(E) u_{l\alpha}^n(r, \mathcal{E}_w^n(E)) Y_{lm}(\widehat{\mathbf{r} - \mathbf{r}_\alpha}) & \mathbf{r} \in MT_\alpha \end{cases} \quad (11)$$

Where

$$\bar{A}_{\mathbf{k}\mathbf{G}}^{lm\alpha n}(E) = \frac{\frac{1}{\sqrt{\Omega}} 4\pi i^l j_l(|\mathbf{k} + \mathbf{G}| S_\alpha) Y_{lm}^*(\widehat{\mathbf{k} + \mathbf{G}})}{u_{l\alpha}^n(S_\alpha, \mathcal{E}_w^n(E))} \quad (12)$$

making the wavefunction continuous. We note that:

$$\Phi_{\mathbf{k}\mathbf{G}}^n(E) = \phi_{\mathbf{k}\mathbf{G}}^n(\mathcal{E}_w^n(E)) \quad (13)$$

We note that  $u_{l\alpha}^n(r, \mathcal{E}_w^n(E)) = u_{l\alpha}^n(r, E_{i,n}^V)$  for some  $E_{i,n}^V$ , so that Eq. (1) need only be solved at a discrete (small) number of energy values to obtain the basis in Eq. (11). Now suppose that for the  $n$ th iteration of the solutions to the KS equations (see Eq. (19) below) we have obtained eigenstates of the KS equations,  $\Psi_{\mathbf{k}\nu}^n$  - with eigenvalues  $\varepsilon_{\mathbf{k}\nu}^n$ , of the form:

$$\Psi_{\mathbf{k}\nu}^n(\mathbf{r}) = \begin{cases} \sum_{\mathbf{G}} \bar{z}_{\mathbf{k}\mathbf{G}}^{\nu n} \frac{1}{\sqrt{\Omega}} \exp(i(\mathbf{k} + \mathbf{G}) \cdot \mathbf{r}) & IR \\ \text{Arbitrary} & MT \end{cases} \quad (14)$$

that is we focus on the expansion of the wavefunction in the IR. Then we that the EWAPW basis for the  $n + 1$ 'st iteration of the solution of the KS equations is given by:

$$\Psi_{\mathbf{k}j}^{n+1} = \sum_{\mathbf{G}} \bar{z}_{\mathbf{k}\mathbf{G}}^{\nu n} \Phi_{\mathbf{k}\mathbf{G}}^{n+1}(\varepsilon_{\mathbf{k}\nu}^n) \quad (15)$$

for  $j = \nu$  (note the similarities with  $(LA)^2 PW$  and in particular  $BEE - (LA)^2 PW$ ). Or in other words  $\bar{O}_{\mathbf{k}\mathbf{G}}^{n+1j} = \bar{z}_{\mathbf{k}\mathbf{G}}^{\nu n}$  (with  $j = \nu$ ) and we augmenting with  $u_{l\alpha}^n(r, \mathcal{E}_w^n(\varepsilon_{\mathbf{k}\nu}^n))$  in the MT. In other words we have that the EWAPW basis is given by:

$$\Psi_{\mathbf{k}j}^{n+1} = \begin{cases} \sum_{\mathbf{G}} \bar{z}_{\mathbf{k}\mathbf{G}}^{\nu n} \frac{1}{\sqrt{\Omega}} \exp(i(\mathbf{k} + \mathbf{G}) \cdot \mathbf{r}) & \mathbf{r} \in IR \\ \sum_{lm} [\sum_{\mathbf{G}} \bar{z}_{\mathbf{k}\mathbf{G}}^{\nu n} A_{\mathbf{k}\mathbf{G}}^{lm\alpha n}(\mathcal{E}_w^n(\varepsilon_{\mathbf{k}\nu}^n))] \times u_{l\alpha}^n(r, \mathcal{E}_w^n(\varepsilon_{\mathbf{k}\nu}^n)) \times Y_{lm}(\widehat{\mathbf{r} - \mathbf{r}_\alpha}) & \mathbf{r} \in MT_\alpha \end{cases} \quad (16)$$

for  $j = \nu$ . We note that Eqs. (16) and (15) are equivalent but in different notation. Or stated even differently we have introduced a basis which is given by the previous eigenstate in the IR and augmented it with the solution of the spherically averaged KS equations at the energy  $\mathcal{E}_w^{n+1}(\varepsilon_{\mathbf{k}\nu}^n)$  in the MT regions.

We notice that the linearization error is at worst given

by:

$$\sim (\varepsilon_{\mathbf{k}\nu}^{n+1} - \mathcal{E}_w^{n+1}(\varepsilon_{\mathbf{k}\nu}^n))^2 \quad (17)$$

When  $\mathcal{E}_w^{n+1}$  is nearly the identity function  $\mathcal{E}_w^{n+1}(\varepsilon_{\mathbf{k}\nu}^n) \cong \varepsilon_{\mathbf{k}\nu}^n$  and the calculations are well converged  $\varepsilon_{\mathbf{k}\nu}^{n+1} \cong \varepsilon_{\mathbf{k}\nu}^n$  this error is small, indeed there are multiple

$E_{i,n}^V$  in the valence and semicore bands so the error  $|\varepsilon_{\mathbf{k}\nu}^n - \mathcal{E}_w^{n+1}(\varepsilon_{\mathbf{k}\nu}^n)|$  is much smaller than bandwidth. We note that given that overall we have created a basis that is given by the previous eigenbasis in the interstitial and augmented it with the eigenstates of the spherically averaged KS Hamiltonian (with the linearization energy relevant of the energies of the previous basis, nearly  $\varepsilon_{\mathbf{k}\nu}^n$  in the limit of many windows) with good convergence between iterations and good spherical symmetry in the MT spheres, in EWAPW, we are working with a basis of near eigenvectors. As such the KS Hamiltonian and overlap matrices will be nearly diagonal and sparse and as such quicker to diagonalize than the LAPW Hamiltonian and overlap matrices. We further note that unlike LAPW or APW+lo we have many radial wavefunctions  $u_{l\alpha}^n(r, E_{i,n}^V)$  per angular momentum channel, it is a comparable or greater amount of radial wavefunctions to LAPW+LO+HDLO+HELO. Furthermore we note that we only have  $N_{\mathbf{G}}$  basis wavefunctions per  $\mathbf{k}$  point. Therefore it is reasonable to surmise that we have a basis with a comparable diagonalization speed to APW and comparable accuracy to LAPW+LO+HDLO+HELO. We note that setting up the KS Hamiltonian, overlap and charge density will take comparable time to setup as in LAPW+LO+HDLO+HELO methods.

### B. Programming Flow

We now show that the code flows, that is the iterative structure of the KS equation remains intact. Suppose we are passed the following data from the previous iteration:  $\{\rho^n(\mathbf{r}), \varepsilon_{\mathbf{k}\nu}^n, \bar{z}_{\mathbf{k}\mathbf{G}}^{\nu n}\}$  that is the electron density, eigenenergies and the decomposition of the eigenstates into plane waves in the interstitial. Now we will show how to pass  $\{\rho^{n+1}(\mathbf{r}), \varepsilon_{\mathbf{k}\nu}^{n+1}, \bar{z}_{\mathbf{k}\mathbf{G}}^{\nu n+1}\}$  to the iteration after thereby making the code flow. To do so, we note that if we form the Hamiltonian and overlap matrices  $H_{jk}^{\mathbf{k}n}$  and  $O_{jk}^{\mathbf{k}n}$  with:

$$\begin{aligned} O_{jk}^{\mathbf{k}n+1} &= \langle \Psi_{\mathbf{k}j}^{n+1} | \Psi_{\mathbf{k}k}^{n+1} \rangle \\ H_{jk}^{\mathbf{k}n+1} &= \int d\mathbf{r} \Psi_{\mathbf{k}j}^{n+1*}(\mathbf{r}) [-\nabla^2 + V_{KS}^{n+1}(\mathbf{r})] \Psi_{\mathbf{k}k}^{n+1}(\mathbf{r}) \\ &\quad + \text{Boundary term} \end{aligned} \quad (18)$$

(see Section IV) then the secular equation is given by:

$$\sum_k H_{jk}^{\mathbf{k}n+1} z_{\mathbf{k}k}^{\nu n+1} = \varepsilon_{\mathbf{k}\nu}^{n+1} \sum_k O_{jk}^{\mathbf{k}n+1} z_{\mathbf{k}k}^{\nu n+1} \quad (19)$$

then we have that

$$\bar{z}_{\mathbf{k}\mathbf{G}}^{\nu n+1} = \sum_k \bar{z}_{\mathbf{k}k}^{\nu n+1} z_{\mathbf{k}\mathbf{G}}^{\mu, n} \quad (20)$$

Where  $\mu = k$  so that we can work in the basis in Eq. (15) and obtain the coefficients  $\bar{z}_{\mathbf{k}\mathbf{G}}^{\nu n+1}$  needed for the next iteration through matrix multiplication. The electron density,  $\rho^{n+1}(\mathbf{r})$ , can be obtained from Section IV.

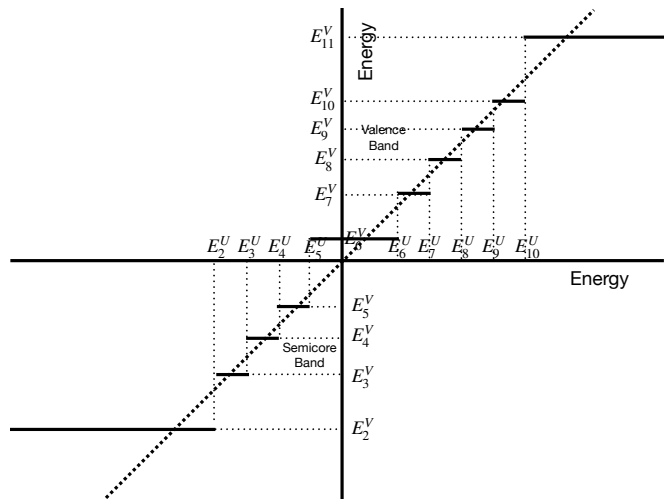


Figure 1. The windowing function  $\mathcal{E}_w(E)$  (solid lines). Notice that the steps become more refined near the valence and semicore bands making  $\mathcal{E}_w(E)$  better approximate the identity function  $Id(E) = E$  in those regions. The identity function is shown for comparison (thick dotted line) and the energies  $E_i^U$  and  $E_i^V$  are also shown. Here we have suppressed the index  $n$  of the iteration of the solution of the KS equations.

### III. COMMENTS

There are many minor technical issues that need to be further handled. Below we describe the solutions to a few of them.

#### A. Initialization

The initialization can be handled in a variety of ways. In one method, the electron density may be chosen as a superposition of electron densities for the various atoms in the system. The initial linearization energy may be the same as in the LAPW or APW+lo basis set whereby we obtain  $\{\rho^1(\mathbf{r}), \varepsilon_{\mathbf{k}\nu}^1, \bar{z}_{\mathbf{k}\mathbf{G}}^{\nu 1}\}$  and then iterate as in Section II B. Alternatively, we can initialize with the set  $\{\rho^0(\mathbf{r}), \varepsilon_{\mathbf{k}\nu}^0, \bar{z}_{\mathbf{k}\mathbf{G}}^{\nu 0}\}$  where  $\rho^0(\mathbf{r})$  is the superposition of the atomic densities and  $\nu = \mathbf{G}$ , with

$$\begin{aligned} \varepsilon_{\mathbf{k}\nu}^0 &= (\mathbf{k} + \mathbf{G})^2 + \bar{V}_{KS}^0 \\ \bar{z}_{\mathbf{k}\mathbf{G}'}^{\nu 0} &= \delta_{\mathbf{G}, \mathbf{G}'} \end{aligned} \quad (21)$$

with  $\nu = \mathbf{G}$ . Here  $\bar{V}_{KS}^0$  is the spatially averaged KS potential.

#### B. Partial Diagonalization

In many situations it is advantageous for computational speed to only look for the lowest few bands and not diagonalize the entire KS Hamiltonian matrix [1].

Indeed the higher bands are unoccupied so do not contribute to the electron density and total energy. In which case since we are interested in only the lowest bands, say only  $\mathcal{M}_{\mathcal{D}}$  of them, we have that the energies  $\varepsilon_{\mathbf{k}\nu}^n, \bar{z}_{\mathbf{k}\mathbf{G}}^{\nu n}$  are computed only with  $\nu \leq \mathcal{M}_{\mathcal{D}}$ . Then for the first  $\mathcal{M}_{\mathcal{D}}$  bands we proceed as in Section II A. The rest of the basis may be obtained as in Eq. (21) with  $0 \leftrightarrow n$  and the  $\mathbf{G}$ 's being chosen such that the smallest  $\mathcal{M}$  energies in Eq. (21) are skipped. That is for the higher  $N_{\mathbf{G}} - \mathcal{M}_{\mathcal{D}}$  bands we write:

$$\begin{aligned} \varepsilon_{\mathbf{k}\nu}^n &= (\mathbf{k} + \mathbf{G})^2 + \bar{V}_{KS}^n \\ \bar{z}_{\mathbf{k}\mathbf{G}'}^{\nu n} &= \delta_{\mathbf{G},\mathbf{G}'} \end{aligned} \quad (22)$$

with  $\nu = \mathbf{G}$ . As such since we have  $\{\rho^n(\mathbf{r}), \varepsilon_{\mathbf{k}\nu}^n, \bar{z}_{\mathbf{k}\mathbf{G}}^{\nu n}\}$  we may generate  $\{\rho^{n+1}(\mathbf{r}), \varepsilon_{\mathbf{k}\nu}^{n+1}, \bar{z}_{\mathbf{k}\mathbf{G}}^{\nu n+1}\}$  and proceed with the iterative solution to the KS equations. This is not a major loss of accuracy as the KS Hamiltonian and overlap matrices are nearly diagonal and sparse and the exact for of the high energy basis does not affect the low energy states significantly.

### C. Expansion of basis set during convergence iteration

In many case it is worthwhile to use small basis sets at the beginning of the convergence loop and larger basis sets later (see [30] and Appendix D). In which case we need to add wavefunctions  $\Phi_{\mathbf{k}\mathbf{G}}^n(E)$  with  $\mathbf{G}_{min}^n < \mathbf{G} < \mathbf{G}_{max}^n$ . These can be added to the main procedure in the same way as described in Section III B.

### D. Partial basis (compatibility with BEE - (LA)<sup>2</sup> PW ideas [19])

Here we note that the number of basis elements  $\Psi_{\mathbf{k}j}^{n+1}$  may be significantly smaller than the value  $N_{\mathbf{G}}$  of reciprocal wavevectors. Indeed once the system has been initialized it is a basis of near eigenvectors it is permissible to significantly reduce basis size. Indeed, as we have a basis of near eigenvectors the Hamiltonian and overlap matrices are nearly diagonal and sparse. As such it is permissible to truncate the basis at much smaller basis numbers than  $N_{\mathbf{G}}$ . We note that this means that in the interstitial we limit ourselves to a smaller basis set but one that is adapted to an earlier IR for an earlier KS Hamiltonian. In principle, to overcome this last minor difficulty [19] we can periodically (every several iterations of the solutions of the KS equations) expand the basis as in Section III C to increase the basis inside the interstitial while still saving on computer time overall. We will call this method BEE-EWAPW [19].

### E. EWAPW vs. Energy Window Linearized Augmented Plane Waves (EWLAPW), multi-radius [30] options.

The EWLAPW basis is described in Appendix A while multi radius options are described in Appendix B (see also ref. [30]). While these methods are slightly advantageous over EWAPW - in that they are slightly more accurate; the added complexity does not seem to be worth the minor improvement. To see this, we notice that the KS Hamiltonian,  $-\nabla^2 + V_{KS}^{n+1}(\mathbf{r})$ , has no singularities on the MT sphere radius. As such the eigenwavefunctions of the KS Hamiltonian should have no singularities near the surface of the MT sphere. Since the basis wavefunctions proposed in EWAPW are near eigenstates they should have no large singularities near the surface of the MT spheres and should be nearly continuously differentiable even though the constituent wavefunctions given in Eq. (11) have derivative discontinuities. As such adding  $u_{l\alpha}^n(r, \mathcal{E}_w^n(\varepsilon_{\mathbf{k}\nu}^n))$  or varying the radius  $S_{\alpha}$  to make the constituent wavefunctions continuously differentiable would not make much of a difference. From another perspective it is true that the scaling of the linearization error improves, we have that the linearization error changes:

$$\sim (\varepsilon_{\mathbf{k}\nu}^{n+1} - \mathcal{E}_w^{n+1}(\varepsilon_{\mathbf{k}\nu}^n))^2 \Rightarrow \sim (\varepsilon_{\mathbf{k}\nu}^{n+1} - \mathcal{E}_w^{n+1}(\varepsilon_{\mathbf{k}\nu}^n))^4, \quad (23)$$

however it is already very small as the basis is nearly complete see Eq. (17) and the discussion below when the bands are well split into multiple windows so the improvement of multi radius and EWLAPW options is minor.

### F. Continuous Interpolation Energy Window Augmented Plane Waves (CEWAPW)

We note that CEWAPW is described in Appendix C. We note that CEWAPW extensions are not essential in the limit of a large number of windows but become more important for a moderate number of windows where they can enhance accuracy at a limited computational cost. We note that continuous interpolation, multi radius and linearization options are combinable with each other.

### G. LO and lo and related extensions

We note that LO and lo extensions as well as HDLO and HELO are not essential. The basis set already has a large number of wavefunctions at various energies of the spherically averaged KS Hamiltonian inside the MT spheres so an additional wavefunction with energy close to those used in the construction of the EWAPW basis would make limited difference - there are already enough radial wavefunction in the EWAPW basis. In principle it is possible to remove some windows around the energies

of the LO wavefunctions and use a larger basis involving LO however that seems disadvantageous. For example, one could remove all the semicore windows; focus on putting many windows in the valence band and add some LO, however there are limited advantages to this. Indeed, this increase of basis set number is not essential for accuracy but is quite detrimental to computational speed (see Section V).

### H. Generating the energy windows

There are many ways to generate energy windows, here we present one scheme, while many others are possible. The idea of this scheme is to divide the occupied states into  $\mathfrak{N}$  pieces and to choose the lowest  $\mathfrak{M}$  unoccupied bands and divide them into  $\mathfrak{P}$  pieces for a total of  $\mathfrak{N} + \mathfrak{P} - 1$  windows. We begin by ordering the eigenvalues  $\varepsilon_{\mathbf{k}\nu}^n \rightarrow \varepsilon^n(M)$  with  $\varepsilon^n(M) \leq \varepsilon^n(M+1)$ ,  $\forall M$ . Now we introduce:

$$N_O^n = \sum_{\mathbf{k}\nu} \Theta(\mu - \varepsilon_{\mathbf{k}\nu}^n) \quad (24)$$

which is the number of occupied states. Here  $\mu$  is the chemical potential. Then for  $i = 2, \dots, \mathfrak{N}$  we have that:

$$E_{i,n+1}^U = \varepsilon^n \left( \frac{i}{\mathfrak{N}} N_O^n \right)$$

$$E_{i,n+1}^V = \frac{\mathfrak{N}}{N_O^n} \sum_{M=\frac{i-1}{\mathfrak{N}} N_O^n}^{\frac{i}{\mathfrak{N}} N_O^n} \varepsilon^n(M) \quad (25)$$

which divide the occupied states into windows (uniformly with respect to number of states occupied per window)

---

Since the EWAPW basis is a basis of near eigenstates of the KS Hamiltonian, the combinations  $\sum_{\mathbf{G}} \tilde{z}_{\mathbf{k}\mathbf{G}}^{\nu n} \exp(i(\mathbf{k} + \mathbf{G}) \cdot \mathbf{r})$  are given by:

$$\sum_{\mathbf{G}} \frac{\tilde{z}_{\mathbf{k}\mathbf{G}}^{\nu n}}{\sqrt{\Omega}} \exp(i(\mathbf{k} + \mathbf{G}) \cdot \mathbf{r}) = 4\pi \sum_{l,m} i^l \left[ \sum_{\mathbf{G}} \frac{\tilde{z}_{\mathbf{k}\mathbf{G}}^{\nu n}}{\sqrt{\Omega}} Y_{lm}^* \left( \widehat{\mathbf{k} + \mathbf{G}} \right) j_l(|\mathbf{k} + \mathbf{G}||\mathbf{r} - \mathbf{r}_\alpha|) \exp(i(\mathbf{k} + \mathbf{G}) \cdot \mathbf{r}_\alpha) \right] Y_{lm} \left( \widehat{\mathbf{r} - \mathbf{r}_\alpha} \right) \quad (29)$$

Whereby we have that

$$\sum_{\mathbf{G}} \frac{\tilde{z}_{\mathbf{k}\mathbf{G}}^{\nu n}}{\sqrt{\Omega}} Y_{lm}^* \left( \widehat{\mathbf{k} + \mathbf{G}} \right) j_l(|\mathbf{k} + \mathbf{G}||\mathbf{r} - \mathbf{r}_\alpha|) \exp(i(\mathbf{k} + \mathbf{G}) \cdot \mathbf{r}_\alpha) \sim \delta_{l,l_0} + \text{corrections} \quad (30)$$

Where  $l_0$  is the dominant angular momentum channel of the band in question. From this we see that only a small number of angular momentum channels participate much like in lo/LO constructions so the truncation angular momentum  $\bar{l}_{max}$  may be reduced. We note that  $\bar{l}_{max} \rightarrow \bar{l}_{max}^{n\mathbf{k}j\alpha}$  can depend on the iteration  $n$ , MT sphere  $\alpha$  and basis wavefunction  $\mathbf{k}j$ .

and places the  $E_{i,n+1}^V$  in the center of mass (with respect to the energy) of those windows. Here  $E_{1,n+1}^U = -\infty$ . While for  $\mathfrak{N} < i < \mathfrak{N} + \mathfrak{P}$  we have that:

$$E_{i,n+1}^U = \varepsilon^n \left( N_O^n + \frac{i - \mathfrak{N}}{\mathfrak{P}} (\mathfrak{M} \cdot N_{\mathbf{k}}) \right)$$

$$E_{i,n+1}^V = \frac{\mathfrak{P}}{\mathfrak{M} \cdot N_{\mathbf{k}}} \sum_{M=N_O^n + \frac{i - \mathfrak{N}}{\mathfrak{P}} (\mathfrak{M} \cdot N_{\mathbf{k}})}^{M=N_O^n + \frac{i - \mathfrak{N} + 1}{\mathfrak{P}} (\mathfrak{M} \cdot N_{\mathbf{k}})} \varepsilon^n(M) \quad (26)$$

which divide the  $\mathfrak{M}$  lowest unoccupied states (uniformly with respect to number of states occupied per window) and places the  $E_{i,n+1}^V$  in the center of mass (with respect to the energy) of those windows. Where

$$N_{\mathbf{k}} = \sum_{\mathbf{k}} 1 \quad (27)$$

is the number of  $\mathbf{k}$  points. With

$$E_{\mathfrak{N}+\mathfrak{P},n+1}^V = \frac{\mathfrak{P}}{\mathfrak{M} \cdot N_{\mathbf{k}}} \sum_{M=N_O^n + \frac{\mathfrak{P}-1}{\mathfrak{P}} (\mathfrak{M} \cdot N_{\mathbf{k}})}^{M=N_O^n + (\mathfrak{M} \cdot N_{\mathbf{k}})} \varepsilon^n(M) \quad (28)$$

while  $E_{\mathfrak{N}+\mathfrak{P},n+1}^U = +\infty$ . Whereby we obtain a specific scheme for generation  $E_{i,n+1}^U$  and  $E_{i,n+1}^V$ , others are also possible.

### I. Reducing the number of angular momentum channels

### J. Reducing the number of radial wavefunctions

In many cases most of the weight of a band in the MT spheres is in the lowest few angular momentum channels. Then it is permissible to handle a certain number of angular momentum channels  $l_{cut} \leq 3$ , or 4 in the EWAPW manner and higher angular momentum channels as in

$(LA)^2 PW$ . We note that  $l_{cut} \rightarrow l_{cut}^{nkj\alpha}$  can depend on the iteration  $n$ , MT sphere  $\alpha$  and basis wavefunction  $\mathbf{k}j$ . This can increase numerical efficiency.

### K. Efficiency of method

We have that the basis size for the EWAPW method is very comparable to that of APW but the construction of the KS Hamiltonian and charge density requires a large number of radial integrals see Eqs. (37) and (51) below. This limits the number of possible windows. However there are many mitigating factors: for a specific  $\mathbf{k}$  point one never needs to consider as many radial wavefunctions as the total number of bands that are considered relevant to the windowing construction (see Section III H for an example of relevant bands where the occupied and lowest  $\mathfrak{M}$  unoccupied bands are relevant so not relevant to the window  $[E_{N-1,n+1}^U, E_{N,n+1}^U = +\infty)$  - in particular one never needs to consider overlap integrals of different energy levels in the same band even if there are several windows per band). Furthermore the number of angular momentum channels  $\bar{l}_{max}^{nkj\alpha}$  is smaller than that for LAPW basis and  $l_{cut}^{nkj\alpha}$ , if introduced, can be quite small thereby reducing the number of needed radial integrals. Furthermore for large scale calculations the diagonalization time is the dominant contribution to the computer time and should be very efficient with the EWAPW basis.

### IV. ENERGY WINDOW FULL POTENTIAL AUGMENTED PLANE WAVES (EWFAPW)

Here we would like to do full potential calculations for the EWAPW basis, or EWFAPW. There are many versions of EWAPW, EWLAPW, CEWAPW, multi radius options, BEE-EWAPW, here we focus on the simplest EWAPW and do not introduce a  $l_{cut}^{nkj\alpha}$ . Extensions to the more involved cases are straightforward but tedious. Here, we break everything (EWFAPW) into simpler pieces - which are easier to code and reuse many pieces of existing codes - which should be evident by comparing this calculation with those of refs. [29, 31–37] for FLAPW. Because the wavefunction and its derivative are nearly continuous near the MT sphere (see Section III E) it is reasonably appropriate to use the Hamiltonian from FLAPW (Eq. (18) without any boundary terms) appropriate to LAPW basis set, however the small corrections to the Hamiltonian due to discontinuity of derivatives of the wavefunction at the MT spheres have been included for accuracy in the form of a boundary term. This correction term comes about because the Laplacian term in the Hamiltonian is not self adjoint when the wavefunctions considered have derivative discontinuities. This may be corrected with a boundary term [2, 23, 28, 38]. Furthermore the small discontinuity of the wavefunction at the MT spheres (due to angular momentum truncation) can also be included [23] in the Hamiltonian. Parts that are

not described namely the Weinert method [39], total energy as well as how to obtain  $V_{KS}^n$  from  $\rho^n(\mathbf{r})$  go over verbatim in our construction from those corresponding to LAPW basis sets, that is that part of FLAPW code can be reused directly [29, 31–37].

### A. Overlap

We write that the overlap is a sum of the overlap when restricting ourselves to the IR plus the sum over the MT spheres:

$$O_{jk}^{kn} = O_{jk}^{knIR} + \sum_{\alpha} O_{jk}^{knMT\alpha} \quad (31)$$

Where  $O_{jk}^{knIR}$  and  $O_{jk}^{knMT\alpha}$  are the IR and MR contributions respectively. Here

$$\begin{aligned} O_{jk}^{knIR} &= \int_{IR} d\mathbf{r} \Psi_{\mathbf{k}j}^{n+1*}(\mathbf{r}) \Psi_{\mathbf{k}k}^{n+1}(\mathbf{r}) \\ O_{jk}^{knMT\alpha} &= \int_{MT\alpha} d\mathbf{r} \Psi_{\mathbf{k}j}^{n+1*}(\mathbf{r}) \Psi_{\mathbf{k}k}^{n+1}(\mathbf{r}) \end{aligned} \quad (32)$$

We now compute  $O_{jk}^{knIR}$  and  $O_{jk}^{knMT\alpha}$  in turn.

#### 1. IR Contribution

We first introduce the function:

$$\Theta^{IR}(\mathbf{r}) = \begin{cases} 1 & \mathbf{r} \in IR \\ 0 & \mathbf{r} \in MT \end{cases} \quad (33)$$

Now we Fourier transform the function in Eq. (33):

$$\begin{aligned} \Theta^{IR}(\mathbf{G}) &\equiv \frac{1}{\Omega} \int d\mathbf{r} \exp(-i\mathbf{G} \cdot \mathbf{r}) \Theta^{IR}(\mathbf{r}) \\ &= \delta_{\mathbf{G},0} - \frac{4\pi}{3\Omega} \sum_{\alpha} \exp(-i\mathbf{G} \cdot \mathbf{r}_{\alpha}) S_{\alpha}^3 \frac{j_1(|\mathbf{G}|S_{\alpha})}{|\mathbf{G}|S_{\alpha}} \end{aligned} \quad (34)$$

Next we define an auxiliary overlap function:

$$\begin{aligned} O_{\mathbf{G}\mathbf{G}'}^{kIR} &= \frac{1}{\Omega} \int_{IR} \exp(-i(\mathbf{G} - \mathbf{G}') \cdot \mathbf{r}) \Theta^{IR}(\mathbf{r}) \\ &= \Theta^{IR}(\mathbf{G} - \mathbf{G}') \end{aligned} \quad (35)$$

Now we have that the overlap in the IR is given in terms of the auxiliary overlap function by:

$$O_{jk}^{knIR} = \sum_{\mathbf{G}, \mathbf{G}'} \bar{o}_{\mathbf{k}\mathbf{G}}^{nj*} \cdot O_{\mathbf{G}\mathbf{G}'}^{kIR} \bar{o}_{\mathbf{k}\mathbf{G}'}^{nk} \quad (36)$$

#### 2. MT Contribution

We introduce the matrix of radial integrals

$$O_{E_{i,n}^V, E_{j,n}^V}^{ln\alpha} = \int_0^{S_{\alpha}} dr \cdot r^2 \cdot u_l^{n\alpha}(r, E_{i,n}^V) \cdot u_l^{n\alpha}(r, E_{j,n}^V) \quad (37)$$

Now using Eqs. (12) and (15) we introduce the constants:

$$C_{klm}^{n\alpha}(k) = \sum_{\mathbf{G}} \bar{o}_{\mathbf{k}\mathbf{G}}^{nk} \cdot A_{\mathbf{k}\mathbf{G}}^{l\alpha n}(\mathcal{E}_w^n(\varepsilon_{\mathbf{k}\nu}^{n-1})) \quad (38)$$

with  $\nu = k$ . Now we have that of the matrix of radial integrals in Eq. (37):

$$O_{jk}^{knIR} = \sum_{lm} C_{klm}^{n\alpha*}(j) O_{\mathcal{E}_w^n(\varepsilon_{\mathbf{k}\nu}^{n-1}), \mathcal{E}_w^n(\varepsilon_{\mathbf{k}\mu}^{n-1})}^{ln\alpha} C_{klm}^{n\alpha}(k) \quad (39)$$

Where  $j = \mu$  and  $k = \nu$ .

## B. Hamiltonian

We write that the Hamiltonian is a sum of the overlap when restricting ourselves to the IR plus the sum over the MT spheres plus a boundary term. The boundary term [2, 23] comes about because we are using wavefunctions which are not continuously differentiable on the MT spheres whereby the Laplacian becomes non-Hermitian and a boundary term is needed in order to fix this prob-

lem [2, 23]. The Hamiltonian is given by:

$$H_{jk}^{kn} = H_{jk}^{knIR} + \sum_{\alpha} H_{jk}^{knMT\alpha} + \sum_{\alpha} H_{jk}^{knBd\alpha} \quad (40)$$

Where  $H_{jk}^{knIR}$ ,  $H_{jk}^{knMT\alpha}$  and  $H_{jk}^{knBd\alpha}$  are the IR, MT and boundary contributions respectively. Here:

$$\begin{aligned} H_{jk}^{knIR} &= \int_{IR} d\mathbf{r} \Psi_{\mathbf{k}j}^{n+1*}(\mathbf{r}) [-\nabla^2 + V_{KS}^n(\mathbf{r})] \Psi_{\mathbf{k}k}^{n+1}(\mathbf{r}) \\ H_{jk}^{knMT\alpha} &= \int_{MT_\alpha} d\mathbf{r} \Psi_{\mathbf{k}j}^{n+1*}(\mathbf{r}) [-\nabla^2 + V_{KS}^n(\mathbf{r})] \Psi_{\mathbf{k}k}^{n+1}(\mathbf{r}) \end{aligned} \quad (41)$$

$H_{jk}^{knIR}$ ,  $H_{jk}^{knMT\alpha}$  and  $H_{jk}^{knBd\alpha}$  (given in Eq. (53) below) in turn. We now write:

$$V_{KS}^n(\mathbf{r}) = \begin{cases} \sum_{\mathbf{G}} V_{KS}^n(\mathbf{G}) \exp(i\mathbf{G} \cdot \mathbf{r}) & \mathbf{r} \in IR \\ \sum_{lm} V_{KS}^{lm\alpha}(r) Y_{lm}(\hat{\mathbf{r}}) & \mathbf{r} \in MT_\alpha \end{cases} \quad (42)$$

### 1. IR Contribution

We now introduce the auxiliary IR Hamiltonian matrix:

$$\begin{aligned} H_{\mathbf{G}\mathbf{G}'}^{knIR} &= \frac{1}{\Omega} \int_{IR} \exp(-i(\mathbf{k} + \mathbf{G}) \cdot \mathbf{r}) [V_{KS}^n(\mathbf{r}) \Theta^{IR}(\mathbf{r}) - \nabla^2 \Theta^{IR}(\mathbf{r})] \exp(i(\mathbf{k} + \mathbf{G}') \cdot \mathbf{r}) \\ &= (V_{KS}^n \Theta^{IR})(\mathbf{G}) + (\mathbf{k} + \mathbf{G}')^2 \Theta^{IR}(\mathbf{G} - \mathbf{G}') \end{aligned} \quad (43)$$

Where by the Fourier multiplication convolution theorem

$$(V_{KS}^n \Theta^{IR})(\mathbf{G}) = \sum_{\mathbf{G}'} V_{KS}^n(\mathbf{G}') \Theta^{IR}(\mathbf{G} - \mathbf{G}') \quad (44)$$

Now we have that the main IR Hamiltonian matrix is given by:

$$H_{jk}^{knIR} = \sum_{\mathbf{G}, \mathbf{G}'} \bar{o}_{\mathbf{k}\mathbf{G}}^{nj*} \cdot H_{\mathbf{G}\mathbf{G}'}^{knIR} \bar{o}_{\mathbf{k}\mathbf{G}'}^{nk} \quad (45)$$

### 2. MT Contribution

The MT contribution may be decomposed into a spherical and non spherical component. We write the spherical harmonics decomposition of the KS Hamiltonian within a MT sphere (see Eq. (42)):

$$-\nabla^2 + V_{KS}^n(\mathbf{r}) = -\nabla^2 + \bar{V}_{KS}^{n\alpha}(r) + \sum_{l \neq 0, m} \bar{V}_{KS}^{lmn\alpha}(r) Y_{lm}(\hat{\mathbf{r}}) \quad (46)$$

Then we write:

$$H_{jk}^{knMT\alpha} = H_{jk}^{knSp\alpha} + H_{jk}^{knNS\alpha} \quad (47)$$

Where:

$$\begin{aligned} H_{jk}^{knSp\alpha} &= \int_{MT_\alpha} d\mathbf{r} \Psi_{\mathbf{k}j}^{n*}(\mathbf{r}) [-\nabla^2 + \bar{V}_{KS}^{n\alpha}(r)] \Psi_{\mathbf{k}k}^n(\mathbf{r}) \\ H_{jk}^{knNS\alpha} &= \int_{MT_\alpha} d\mathbf{r} \Psi_{\mathbf{k}j}^{n*}(\mathbf{r}) \sum_{l \neq 0, m} \bar{V}_{KS}^{lmn\alpha}(r) Y_{lm}(\hat{\mathbf{r}}) \Psi_{\mathbf{k}k}^n(\mathbf{r}) \end{aligned}$$

*Spherical Component* We first note that:

$$\begin{aligned} H_{jk}^{knSp\alpha} &= \int_{MT_\alpha} d\mathbf{r} \Psi_{\mathbf{k}j}^{n*}(\mathbf{r}) [-\nabla^2 + \bar{V}_{KS}^{n\alpha}(r)] \Psi_{\mathbf{k}k}^n(\mathbf{r}) \\ &= \int_{MT_\alpha} d\mathbf{r} \Psi_{\mathbf{k}j}^{n*}(\mathbf{r}) E_{i,n}^V \Psi_{\mathbf{k}k}^n(\mathbf{r}) \end{aligned} \quad (48)$$

for some  $i$ . We now introduce the matrix of Hamiltonian radial overlaps:

$$H_{E_{i,n}^V, E_{j,n}^V}^{ln\alpha} \equiv E_{j,n}^V \cdot O_{E_{i,n}^V, E_{j,n}^V}^{ln\alpha} \quad (49)$$

We now use Eq. (1) to write that the spherical component of the Hamiltonian is given by:

$$H_{jk}^{\mathbf{k}nSp\alpha} = \sum_{lm} C_{\mathbf{k}lm}^{n\alpha*}(j) H_{\mathcal{E}_w^n(\varepsilon_{\mathbf{k}\nu}^{n-1}), \mathcal{E}_w^n(\varepsilon_{\mathbf{k}\mu}^{n-1})}^{ln\alpha} C_{\mathbf{k}lm}^{n\alpha}(k) \quad (50)$$

Where  $j = \nu$  and  $k = \mu$ .

*Non-Spherical Component* We now introduce the functions:

$$\begin{aligned} G_{l,l',l''}^{m,m',m''} &= \int Y_{lm}^* Y_{l'm'} Y_{l''m''} d\Omega, \\ H_{E_{i,n}^V, E_{j,n}^V}^{ll'm',l''n\alpha} &= \int_0^{S_\alpha} dr \cdot r^2 \cdot u_l^{n\alpha}(r, E_{i,n}^V) \times \\ &\quad \times \bar{V}_{KS}^{lmn\alpha}(r) \cdot u_{l''}^{n\alpha}(r, E_{j,n}^V) \end{aligned} \quad (51)$$

---


$$H_{jk}^{\mathbf{k}nNS\alpha} = \sum_{lm, l' \neq 0m', l''m''} C_{\mathbf{k}lm}^{n\alpha*}(j) G_{l,l',l''}^{m,m',m''} H_{\mathcal{E}_w^n(\varepsilon_{\mathbf{k}\nu}^{n-1}), \mathcal{E}_w^n(\varepsilon_{\mathbf{k}\mu}^{n-1})}^{ll'm',l''n\alpha} C_{\mathbf{k}l''m''}^{n\alpha}(k) \quad (52)$$

Where  $j = \nu$  and  $k = \mu$ .

---

### 3. Boundary Contribution

We have that [2, 23]:

$$H_{jk}^{\mathbf{k}nBd\alpha} = \int_{\partial MT_\alpha} d\mathbf{r} \Psi_{\mathbf{k}j}^n(\mathbf{r}) \left[ \frac{\partial}{\partial r_1} - \frac{\partial}{\partial r_2} \right] \Psi_{\mathbf{k}k}^n(\mathbf{r}) \quad (53)$$

Where  $\partial MT_\alpha$  is the surface of the  $\alpha$ 'th MT sphere and  $\frac{\partial}{\partial r_1}, \frac{\partial}{\partial r_2}$  refer to derivatives at the inner and outer boundaries. We now introduce the auxiliary function:

---


$$\begin{aligned} H_{\mathbf{G}, E_{i,n}^V, \mathbf{G}'}^{\mathbf{k}lmnBd\alpha} &= \frac{4\pi}{\sqrt{\Omega}} \exp(i(\mathbf{k} + \mathbf{G}) \cdot \mathbf{r}_\alpha) Y_{lm}^* \left( \widehat{\mathbf{k} + \mathbf{G}} \right) i^l j_l (|\mathbf{k} + \mathbf{G}| S_\alpha) \times \\ &\quad \times \left[ \bar{A}_{\mathbf{k}\mathbf{G}'}^{lm\alpha n}(E_{i,n}^V) \frac{\partial}{\partial r} u_{l\alpha}^n(E_{i,n}^V, r)_{r=S_\alpha} - \frac{4\pi}{\sqrt{\Omega}} \exp(i(\mathbf{k} + \mathbf{G}') \cdot \mathbf{r}_\alpha) Y_{lm}^* \left( \widehat{\mathbf{k} + \mathbf{G}'} \right) i^l \frac{\partial}{\partial r} j_l (|\mathbf{k} + \mathbf{G}'| r)_{r=S_\alpha} \right] \end{aligned} \quad (54)$$

Then we have that:

$$H_{jk}^{\mathbf{k}nBd\alpha} = \sum_{lm} \sum_{\mathbf{G}, \mathbf{G}'} \bar{o}_{\mathbf{k}\mathbf{G}}^{nj*} \cdot H_{\mathbf{G}, \mathcal{E}_w^n(\varepsilon_{\mathbf{k}\nu}^{n-1}), \mathbf{G}'}^{\mathbf{k}lmnBd\alpha} \cdot \bar{o}_{\mathbf{k}\mathbf{G}'}^{nk} \quad (55)$$

Where  $j = \nu$ .

### C. Electron density

We would like to write the electron density in the standard form:

$$\rho^n(\mathbf{r}) = \begin{cases} \sum_{\mathbf{G}} \rho^n(\mathbf{G}) \cdot \exp(i\mathbf{G} \cdot \mathbf{r}) & \mathbf{r} \in IR \\ \sum_{lm} \rho_{lm}^{n\alpha}(r) Y_{lm} \left( \widehat{\mathbf{r} - \mathbf{r}_\alpha} \right) & \mathbf{r} \in MT_\alpha \end{cases} \quad (56)$$

Which is useful for the Weinert method [39] and the calculation of  $V_{KS}^n(\mathbf{r})$  from  $\rho^n(\mathbf{r})$  [23].

### 1. IR Component

We first introduce the matrices:

$$Z_{\mathbf{kG}\nu}^n = \sum_j \bar{a}_{\mathbf{kG}}^{nj} \cdot \bar{z}_{\mathbf{kj}}^{\nu n} \quad (57)$$

Which give the expansion in terms of plane waves of the eigenfunctions of the KS Hamiltonian. Then we have that

$$\rho^n(\mathbf{G}) = 2 \sum_{\mathbf{k}} \sum_{\nu} f(\varepsilon_{\mathbf{k}\nu}^n) \sum_{\mathbf{G}'} Z_{\mathbf{kG}\nu}^{n*} Z_{\mathbf{k}(\mathbf{G}+\mathbf{G}')\nu}^n \quad (58)$$

The factor of 2 comes from spin degeneracy.

### 2. MT Component

We now introduce the auxiliary matrices:

$$C_{\mathbf{k}lm}^{\nu n\alpha}(j, r) = \bar{z}_{\mathbf{kj}}^{\nu n} \cdot C_{\mathbf{k}lm}^{n\alpha}(j) u_{l\alpha}^n \left( r, \mathcal{E}_w^n \left( \varepsilon_{\mathbf{k}\mu}^{n-1} \right) \right) \quad (59)$$

With  $\mu = j$ . Then we have that:

$$\begin{aligned} \rho_{lm}^{n\alpha}(r) &= 2 \sum_{\mathbf{k}} \sum_{\nu} f(\varepsilon_{\mathbf{k}\nu}^n) \times \\ &\times \sum_{jk} \sum_{l'm'} \sum_{l''m''} C_{\mathbf{k}l'm'}^{\nu n\alpha*}(j, r) C_{\mathbf{k}l''m''}^{\nu n\alpha}(k, r) G_{l''l'}^{m'',m'} \end{aligned} \quad (60)$$

## V. DISCUSSIONS & CONCLUSIONS

In this work we introduced a new method to solve the KS problem once the form of the correlation and exchange piece of the KS potential (be it within the Local Density Approximation (LDA), Generalized Gradient Approximation (GGA), metaGGA etc. [40–44]) has been fixed. In our method, EWAPW, we use the fact that solving the KS equations is an iterative process and use previous iteration's eigenstate and eigenvalue information to produce a new basis for each iteration of the solution of the KS equations (see Section II A). We have argued that no LO/lo or extensions (such as semicore LO, HDLO, HELO...) would not significantly improve the accuracy of the solution as we have many linearization energies per occupied band (and a few for the unoccupied ones). As such we have created a competitor for LAPW+LO (as well as LAPW+HDLO, LAPW+HELO, LAPW+HDLO+HELO, etc.). However the basis set size we use is significantly smaller than LO type extensions as we have one or even less (see Section III D) eigenstate per reciprocal lattice vector  $\mathbf{G}$ . This is an important advantage; indeed typical DFT calculations use 80-100  $\mathbf{G}$  vectors per atom for large MT spheres [9, 19], while LO in the  $s$ ,  $p$ ,  $d$ ,  $f$  or even  $g$  channels (for high accuracy) gives an additional 16-25 additional basis functions per

LO band, so if we have LAPW+LO+HDLO+HELO( $\times 3$ ) [7, 19, 24] (where the ( $\times 3$ ) indicates three HELO bands are introduced) which is likely to have comparable accuracy to EWAPW methods, as it uses a comparable number of radial wavefunctions per atom, we can easily need to generate an additional 80-125 basis functions per atom. Doubling the basis size increase work load for diagonalization by a factor of  $\sim$ eight so EWAPW is highly advantageous. Furthermore the Hamiltonian and overlap matrices for EWAPW are nearly diagonal and sparse giving additional speedup. In other words we have produced a basis with the efficiency of the APW basis but with accuracy of LAPW+LO+HDLO+HELO. We would like to note that the efficiency of a DFT method is mostly determined by the efficiency of the diagonalization process and the efficiency of setting up the KS Hamiltonian, overlap matrix and charge distribution. While the EWAPW basis has the efficiency of diagonalization of APW or better (same basis size, but a sparser matrix) EWAPW takes comparable time to LAPW+LO+HDLO+HELO to set up the KS Hamiltonian and overlap matrices as well as the electron density because of the many radial wavefunctions involved.

In this paper we focused on a specific method EWAPW, however as we discussed there are many variations of this method BEE-EWAPW, EWLAPW, multi radius and CEWAPW options. Furthermore there are many somewhat different ways of choosing the windowing function; CEWAPW has several variations and it is possible to introduce a  $l_{cut}^{nkj\alpha}$ . While we have argued that there will not be a very significant change between all these methods, with respect to the accuracy of the solution of the KS problem - especially for a large number of windows, in the future it would still be of great interest to optimize the time requirements and the accuracy with respect to all these variations of the main method. Also in the future it would be of interest to combine these methods (EWAPW and related) with Hartree Fock as in DFT+U [45], or Dynamical Mean Field Theory [46], DFT+DMFT [45], or Gutzwiller Approximation, DFT+GA [47] to obtain more accurate results for strongly correlated systems. It would also be of interest to include magnetism, superconductivity and relativistic effects for enhanced accuracy, as well as to extend the results to thin films. Besides expanding the methods it would also be of interest to expand applications, namely forces (including the Pulay contribution - which we believe to be very small in this case as the basis is nearly complete [49]), pressure and stress [48, 50]. As well as introduce DFT perturbation theory and study phonons with various methods [48]. This can be done for a large variety of options of EWAPW for DFT, DFT+U, DFT+DMFT, DFT+GA. We would also like to expand EWAPW to Energy Window Muffin Tin Orbitals (EWMTO [51]) and to energy window pseudopotential methods. This would greatly increase the applicability of energy window methods. Overall it would be of great interest to apply EWAPW to real ma-

terials.

### Appendix A: EWLAPW

Here we briefly describe EWLAPW, which is similar to EWAPW. We now introduce:

$$\Psi_{\mathbf{kG}}^{Ln}(E) = \begin{cases} \frac{1}{\sqrt{\Omega}} \exp(i(\mathbf{k} + \mathbf{G}) \cdot \mathbf{r}) & \mathbf{r} \in IR \\ [a_{\mathbf{k}+\mathbf{G}}^{L\alpha n}(\mathcal{E}_w(E)) u_{l\alpha}^n(r, \mathcal{E}_w^{Ln}(E)) + b_{\mathbf{k}+\mathbf{G}}^{L\alpha n}(\mathcal{E}_w(E)) \dot{u}_{l\alpha}^n(r, \mathcal{E}_w^{Ln}(E))] Y_{lm}(\widehat{\mathbf{r} - \mathbf{r}_\alpha}) & \mathbf{r} \in MT_\alpha \end{cases} \quad (\text{A1})$$

Where the wavefunction is continuous and continuously differentiable. We also note that:

$$\Psi_{\mathbf{kG}}^{Ln}(E) = \phi_{\mathbf{kG}}^{Ln}(\mathcal{E}_w(E)) \quad (\text{A2})$$

Where we have introduced a windowing function  $\mathcal{E}_w^{Ln}(E)$  which is given by:

$$\mathcal{E}_w^{Ln}(E) = \sum_{i=2}^N E_{i,n}^{LV} \cdot (\Theta(E - E_{i-1,n}^{LU}) - \Theta(E - E_{i,n}^{LU})) \quad (\text{A3})$$

Where  $E_{1,n}^{LU} = -\infty$ ,  $E_{N,n}^{LU} = +\infty$  and  $E_{i-1,n}^{LU} < E_{i,n}^{LU} < E_{i,n}^{LV} \forall i$ . Now suppose that for the  $n$ th step in the solutions to the KS equations we have a basis of the form:

$$\Psi_{\mathbf{k}\nu}^{Ln}(\mathbf{r}) = \begin{cases} \sum_{\mathbf{G}} z_{\mathbf{kG}}^{L\nu n} \frac{1}{\sqrt{\Omega}} \exp(i(\mathbf{k} + \mathbf{G}) \cdot \mathbf{r}) & IR \\ \text{Arbitrary} & MT \end{cases} \quad (\text{A4})$$

for some  $E_{i,n}^{LV}$ . Then we that

$$\Psi_{\mathbf{k}j}^{Ln+1} = \sum_{\mathbf{G}} z_{\mathbf{kG}}^{L\nu n} \Psi_{\mathbf{kG}}^{Ln+1}(\varepsilon_{\mathbf{k}\nu}^{Ln}) \quad (\text{A5})$$

for  $j = \nu$  and  $\varepsilon_{\mathbf{k}\nu}^{Ln}$  are eigenvalues of the  $n$ 'th iteration of EWLAPW. The rest is very similar to EWPAW.

### Appendix B: Multi Radius options

Consider the following wave functions, which are similar to the Soler-Williams construction [5, 6]:

$$\begin{aligned} \check{\Psi}_{\mathbf{kG}}^n(E) &= \frac{1}{\sqrt{\Omega}} \exp(i(\mathbf{k} + \mathbf{G}) \cdot \mathbf{r}) + \\ &+ \sum_{\alpha} \sum_{l,m} Y_{lm}(\widehat{\mathbf{r} - \mathbf{r}_\alpha}) \left[ \check{A}_{\mathbf{k}+\mathbf{G}}^{l\alpha n}(E) u_{l\alpha}^n(r, \mathcal{E}_w^n(E)) - \frac{4\pi}{\sqrt{\Omega}} i^l Y_{lm}^*(\widehat{\mathbf{k} + \mathbf{G}}) \exp(i(\mathbf{k} + \mathbf{G}) \cdot \mathbf{r}_\alpha) j_l(|\mathbf{k} + \mathbf{G}| |\mathbf{r} - \mathbf{r}_\alpha|) \right] \times \\ &\times \Theta(S_\alpha^l(|\mathbf{k} + \mathbf{G}|) - |\mathbf{r} - \mathbf{r}_\alpha|) \end{aligned} \quad (\text{B1})$$

Here we have subtracted out the part of the plane wave inside the MT sphere, in the second term of the second line of Eq. (B1), that is decomposed it as in Eq. (3) into Bessel functions times spherical harmonics and subtracted them piece by piece from the solutions of the exact radially symmetric KS equations. We note that these wavefunctions are well defined even when the MT spheres, with radii  $S_\alpha^l(|\mathbf{k} + \mathbf{G}|)$ , are such that the MT spheres overlap. Notice that there are different radii for different angular momentum channels and different magnitudes of wavevector  $|\mathbf{k} + \mathbf{G}|$ . We also

choose the coefficients  $\check{A}_{\mathbf{k}+\mathbf{G}}^{l\alpha n}$  to be given by a relation similar to Eq. (12) such that the wave function is continuous at  $S_\alpha^l(|\mathbf{k} + \mathbf{K}|)$ . Now we choose  $S_\alpha^l(|\mathbf{k} + \mathbf{K}|)$  such that the wave function is also continuously differentiable at  $S_\alpha^l(|\mathbf{k} + \mathbf{K}|)$  (this may be done by a root finding procedure [30]). We now repeat the arguments in Section II with  $\Psi_{\mathbf{kG}}^n(E) \rightarrow \check{\Psi}_{\mathbf{kG}}^n(E)$  to obtain a basis set procedure. We note that the linearization error goes as  $\sim (\varepsilon_{\mathbf{k}\nu}^{n+1} - \mathcal{E}_w(\varepsilon_{\mathbf{k}\nu}^n))^4$  [1, 2, 30] instead of  $\sim (\varepsilon_{\mathbf{k}\nu}^{n+1} - \mathcal{E}_w(\varepsilon_{\mathbf{k}\nu}^n))^2$  despite having APW basis set that is no terms proportional to  $\dot{u}_{l\alpha}^n(r, \mathcal{E}_w^n(E))$  [30]. Indeed

by matching the derivative we have essentially studied the case when there is  $\dot{u}_{l\alpha}^n(r, \mathcal{E}_w^n(E))$  (it is included) and we found that the coefficient in front of it is zero at that

radius [30].

### Appendix C: CEWAPW

CEWAPW is based on the following wavefunctions:

$$\begin{aligned} \tilde{\Phi}_{\mathbf{k}\mathbf{G}}^n(E) = & \sum_{i=3}^{N-1} \left[ \frac{\phi_{\mathbf{k}\mathbf{G}}^n(E_{i-1,n}^{CU})(E_{i,n}^{CU} - E) + \phi_{\mathbf{k}\mathbf{G}}^n(E_{i,n}^{CU})(E - E_{i-1,n}^{CU})}{E_{i,n}^{CU} - E_{i-1,n}^{CU}} \right] \cdot (\Theta(E - E_{i-1,n}^{CU}) - \Theta(E - E_{i,n}^{CU})) \\ & + \phi_{\mathbf{k}\mathbf{G}}^n(E_{2,n}^{CU})\Theta(E_{2,n}^{CU} - E) + \phi_{\mathbf{k}\mathbf{G}}^n(E_{N-1,n}^{CU})\Theta(E - E_{N-1,n}^{CU}) \end{aligned} \quad (C1)$$

Where  $E_{1,n}^{CU} = -\infty$ ,  $E_{N,n}^{CU} = +\infty$  and  $E_{i-1,n}^{CU} < E_{i,n}^{CU} \forall i$ . These wavefunctions continuously interpolate between the various wavefunctions  $\phi_{\mathbf{k}\mathbf{G}}^n(E_{i,n}^{CU})$ . One then replaces  $\tilde{\Phi}_{\mathbf{k}\mathbf{G}}^n(E) \leftrightarrow \Phi_{\mathbf{k}\mathbf{G}}^n(E)$  in Section II A and proceeds to build a basis of near eigenstates. Alternatively one could use even more sophisticated interpolation schemes and write  $\hat{\Phi}_{\mathbf{k}\mathbf{G}}^n(E) =$ :

$$\begin{aligned} \sum_{i=2}^{N-1} \phi_{\mathbf{k}\mathbf{G}}^n(E_{i,n}^{CU}) \prod_{j \neq i} \frac{(E - E_{j,n}^{CU})}{(E_{i,n}^{CU} - E_{j,n}^{CU})} \Theta(E_{N-1,n}^{CU} - E) + \\ + \phi_{\mathbf{k}\mathbf{G}}^n(E_{N-1,n}^{CU}) \Theta(E - E_{N-1,n}^{CU}) \end{aligned} \quad (C2)$$

One then replaces  $\hat{\Phi}_{\mathbf{k}\mathbf{G}}^n(E) \leftrightarrow \Phi_{\mathbf{k}\mathbf{G}}^n(E)$  in Section II A and proceeds to build a basis of near eigenstates. In general any reasonable linear interpolation method, that sends the constant sequence to a constant function function, would do. We note that:

$$\begin{aligned} \sum_{i=2}^{N-1} \frac{1}{\sqrt{\Omega}} \exp(i(\mathbf{k} + \mathbf{G}) \cdot \mathbf{r}) \prod_{j \neq i} \frac{(E - E_{j,n}^{CU})}{(E_{i,n}^{CU} - E_{j,n}^{CU})} \\ = \frac{1}{\sqrt{\Omega}} \exp(i(\mathbf{k} + \mathbf{G}) \cdot \mathbf{r}) \end{aligned} \quad (C3)$$

So that

$$\hat{\Phi}_{\mathbf{k}\mathbf{G}}^n(E) = \frac{1}{\sqrt{\Omega}} \exp(i(\mathbf{k} + \mathbf{G}) \cdot \mathbf{r}) \quad (C4)$$

for  $\mathbf{r} \in IR$ .

### Appendix D: Adjusting the basis set size with iteration (review)

Most current DFT calculations for crystalline solids introduce a discrete basis set with the basis set often being indexed by  $\mathbf{k}, \mathbf{G}$  and for practical reasons is limited to  $\mathbf{G} < \mathbf{G}_{max}$ , while  $\mathbf{k}$  is on a discrete grid. Typically several hundred  $\mathbf{k}$  points are taken and roughly 80-100 reciprocal lattice vectors,  $\mathbf{G}$  points, per atom [1, 19] are

used for the case of large MT spheres. In many DFT calculations the dominant contribution to computational time is solving Eq. (19) for a total of  $\mathcal{N}$  times till convergence with each run taking  $\sim \mathbf{G}_{max}^9$  time for a total of  $\sim \mathcal{N} \mathbf{G}_{max}^9$  computations. Here  $\mathcal{N} \sim 20$  for many situations [19]. Now at each step from numerical simulations it is known that the error from an exact solution the KS equations is given by [1, 9, 19, 52]:

$$\Delta \varepsilon \sim [\varepsilon_n \exp(-An^\alpha) + \varepsilon_{\mathbf{G}} \exp(-B\mathbf{G}_{max}^\beta)] \quad (D1)$$

For  $\varepsilon_n \sim \varepsilon_{\mathbf{G}} \lesssim 1$  Ry. Furthermore in many cases  $\alpha \cong \beta \cong 1$  - [19, 52]. This shows that the scaling of the computation time  $\sim \mathcal{N} \mathbf{G}_{max}^9$  is very wasteful as for small  $n$  there is no point in using as large a  $\mathbf{G}_{max}$ . Here we propose to introduce a  $\mathbf{G}_{max}(n)$  where

$$B\mathbf{G}_{max}^\beta(n) \sim An^\alpha \Rightarrow \mathbf{G}_{max}(n) \sim \left(\frac{A}{B}\right)^{1/\beta} n^{\alpha/\beta} \quad (D2)$$

We also want  $\mathbf{G}_{max}(\mathcal{N}) = \mathbf{G}_{max}$ . This gives us a first approximation that

$$\mathbf{G}_{max}(n) \sim \mathbf{G}_{max} \left(\frac{n}{\mathcal{N}}\right)^{\alpha/\beta} \quad (D3)$$

As such  $\mathbf{G}_{max}(\mathcal{N} - n) = \mathbf{G}_{max} \left(\frac{\mathcal{N} - n}{\mathcal{N}}\right)^{\alpha/\beta} = \mathbf{G}_{max} \left(1 - \frac{n}{\mathcal{N}}\right)^{\alpha/\beta} = \mathbf{G}_{max} \exp\left(-\frac{\alpha}{\beta} \frac{n}{\mathcal{N}}\right)$  computational time will then scale as:

$$\begin{aligned} T \sim \sum_n \mathbf{G}_{max}^9(\mathcal{N} - n) \sim \int_{-\infty}^0 dt \mathbf{G}_{max}^9 \exp\left(-9\frac{\alpha}{\beta} \frac{t}{\mathcal{N}}\right) \\ \Rightarrow T \sim \mathbf{G}_{max}^9 \left[\frac{\mathcal{N}\beta}{9\alpha} + 1\right] \end{aligned} \quad (D4)$$

Where we have estimated the last iteration loop more carefully as it is often important (hence  $\frac{\mathcal{N}\beta}{9\alpha} \rightarrow \frac{\mathcal{N}\beta}{9\alpha} + 1$ ). This leads to a computational improvement of the scale of  $\sim \frac{\mathcal{N}}{\frac{\mathcal{N}\beta}{9\alpha} + 1}$  on top of those described in the main text. We note that it is also possible to modify the  $\mathbf{k}$  space mesh to be more refined for large  $n$  thereby saving

further computer time, this works with a variety of solid state DFT methods including EWAPW. Furthermore, for EWAPW it is possible to increase the number of windows with convergence iterations thereby saving on EWFAPW time on top of the previous time saving modifications.

We further note that for calculations with LO/lo type wavefunctions (likely not relevant to EWAPW) it can be advantageous to increase the amount of LO/lo basis elements with convergence iterations.

- 
- [1] D. J. Singh and D. Nordstrom, *Planewaves, pseudopotentials, and the LAPW method* (Springer, New York, 2006).
- [2] R. M. Martin, *Electronic Structures Basic Theory and Practical Methods* (Cambridge University Press, Cambridge, 2020).
- [3] D. Marx and J. Hutter, *Ab Initio Molecular Dynamics Basic Theory and Advanced Methods* (Cambridge University Press, Cambridge, 2009).
- [4] O. K. Andersen, Phys. Rev. B **12**, 3060 (1975).
- [5] J. M. Soler, and A. R. Williams, Phys. Rev. B **40**, 1560 (1989).
- [6] J. M. Soler and A. R. Williams, Phys. Rev. B **42**, 9728 (1990).
- [7] G. Michalíček, M. Betzinger, C. Friedrich and S. Blügel, Comp. Phys. Comm. **184**, 2670 (2013).
- [8] D. J. Singh, Phys. Rev. B **43**, 6388 (1991).
- [9] E. Sjöstedt, L. Nordstrom, and D. J. Singh, Sol. Sta. Comm. **114**, 15 (2000).
- [10] D. D. Koeling and G. O. Arbam, J. Phys. F: Met. Phys. **5**, 2041 (1975).
- [11] J. M. Wills, M. Alouani, P. Anderson, A. Dellin, O. Eriksson, and O. Grechnev, *Full-Potential Electronic Structure Method Energy and Force Calculations with Density Functional Theory and Dynamical Mean Field Theory* (Springer, New York, 2010).
- [12] H. L. Skriver, *The LMTO method Muffin-Tin Orbitals and Electronic Structure* (Springer, New York, 1984).
- [13] O. K. Andersen, and O. Jepsen, Phys. Rev. Lett. **53**, 2571 (1984).
- [14] O. K. Andersen, T. S.-Dasgupta, and S. Ezhof, Bull. Mat. Sci. **26**, 19 (2003).
- [15] W. Kohn, N. Rostoker, Phys. Rev. **94**, 1111 (1954).
- [16] J. Koringa, Physica **13**, 392 (1947).
- [17] D. Vanderbilt, Phys. Rev. B **41**, 7892 (1990).
- [18] P. E. Blochl, Phys. Rev. B **50**, 17953 (1994).
- [19] G. Michalíček, *Extending the precision and efficiency of all-electron full-potential linearized augment plane-wave density functional theory* (Aachen University, 2014, thesis).
- [20] J. C. Slater, Phys. Rev. **51**, 846 (1937).
- [21] L. Smrčka, Czech. J. of Phys. **34**, 694 (1984).
- [22] J. Petrů and L. Smrčka, Czech. J. of Phys. **35**, 62 (1985).
- [23] T. L. Loucks, *Augmented Plane Wave Method* (W. A. Benjamin Inc., New York, 1967).
- [24] A. L. Kutepov, Phys. Rev. B **103**, 165101 (2021).
- [25] C. Friedrich, A. Schindlmayr, S. Blügel, T. Kotani, Phys. Rev. B **74**, 045104 (2006).
- [26] M. Betzinger, C. Friedrich, S. Blügel, A. Görling, Phys. Rev. B **83**, 045105 (2011).
- [27] G. K. H. Madsen, P. Blaha, K. Schwarz, E. Sjöstedt, and L. Nordström, Phys. Rev. B **64**, 195134 (2001).
- [28] E. Sjöstedt, Licantiate thesis (Uppsala University, 1999, Sweden).
- [29] S. Blügel and G. Bihlmayer, *Full-Potential Linearized Augmented Plane Wave Method in Computational Nanoscience: Do it yourself!*, J. Grotendorst, S. Blügel and D. Marx (Eds.) (John von Neumann Institute for Computing, Jülich, 2006).
- [30] G. Goldstein, arXiv 2403.15954.
- [31] D. R. Hamann, Phys. Rev. Lett. **42**, **662** (1979).
- [32] E. Wimmer, H. Krakauer, M. Weinert and A. J. Freeman, Phys. Rev. B **24**, 864 (1981).
- [33] H. J. F. Jansen and A. J. Freeman, Phys. Rev. B **30**, 561 (1984).
- [34] S.-H. Wei, and H. Krakauer, Phys. Rev. Lett. **55**, 1200 (1985).
- [35] S.-H. Wei, H. Krakauer and M. Weinert, Phys. Rev. B **32**, 7792 (1985).
- [36] L. F. Mattheis, and D. R. Hamann, Phys. Rev. B **33**, 823 (1986).
- [37] P. Blaha, K. Schwarz, P. Sorantin, and S. B. Trickey, Comp. Phys. Comm. **59**, 399 (1990).
- [38] P. M. Marcus, Int. J. Quantum Chem. **1S**, 567 (1967).
- [39] M. Weinert, J. Math. Phys. **22**, 2433 (1981).
- [40] E. Engel and R. M. Dreizler, *Density Functional Theory: An Advanced Course* (Springer, 2011, Berlin Heidelberg).
- [41] H. Eschrig, *The Fundamentals of Density Functional Theory* (B. G. Teubner, 1996, Leipzig).
- [42] W. Koch and M. C. Holthausen, *A Chemist's Guide to Density Functional Theory* (Wiley-WCH, 2001, Weinheim).
- [43] R. M. Dreizler and E. K. U. Gross, *Density Functional Theory: An Approach to the Quantum Many-Body Problem* (Springer, 1990, Berlin Heidelberg).
- [44] T. Tsuneda, *Density Functional Theory in Quantum Chemistry* (Springer, 2014, Japan).
- [45] G. Kotliar, S. Y. Savrasov, K. Haule, V. S. Oudovenko, O. Parcollet, C. A. Marianetti, Rev. Mod. Phys. **78**, 865 (2006).
- [46] A. Georges, G. Kotliar, W. Krauth and M. J. Rozenberg, Rev. Mod. Phys. **68**, 13 (1996).
- [47] N. Lanata, Y. Yao, C.-Z. Wang, K.-M. Ho and G. Kotliar, Phys. Rev. X **5**, 011008 (2015).
- [48] D. A. Klüppelberg, *First Principles Investigation of Displacive Response in Complex Solids* (Jülich, 2015, thesis).
- [49] R. Yu, D. Singh and H. Krakauer, Phys. Rev. B **43**, 6411 (1991).
- [50] K. Belbase, A. Tröster and P. Blaha, Phys. Rev. B **104**, 174113 (2021).
- [51] G. Goldstein, arXiv 2407.15299.
- [52] N. D. Woods, M. C. Payne and P. J. Haspin, J. Phys. Cond. Matter **31**, 453001 (2019).